Published in final edited form as:
Invest Ophthalmol Vis Sci. 2007 December ; 48(12): 5788–5797.

The Oscillatory Potentials of the Dark-Adapted Electroretinogram in Retinopathy of Prematurity

James D. Akula[1], **Julie A. Mocko**[1,2], **Anne Moskowitz**[1], **Ronald M. Hansen**[1], and **Anne B. Fulton**[1]

1 *Department of Ophthalmology, Children's Hospital Boston and Harvard Medical School, Boston, Massachusetts*

2 *Department of Behavioral Neuroscience, Northeastern University, Boston, Massachusetts*

Abstract

Purpose—To study the development of the electroretinographic (ERG) oscillatory potentials (OPs) in two rat models of ROP and in human subjects with a history of ROP.

Methods—Sprague-Dawley rats (n = 36) were studied longitudinally. Rat models of ROP were induced, either by exposure to alternating 50%/10% oxygen (50/10 model) from postnatal day (P) 0 to P14 or by exposure to 75% oxygen (75 model) from P7 to P14. Control rats were reared in room air. Infant and adult human subjects with and without a history of ROP (n = 91) were also studied. Dark-adapted ERGs were recorded and filtered to demonstrate the OPs. Discreet Fourier transform (DFT) allowed evaluation of the OP power spectrum. OP energy (E), dominant frequency (F_{peak}), and sensitivity (log $i_{1/2}$) were evaluated.

Results—In 50/10 model rats, E was low compared with that in the 75 model rats and control animals. F_{peak} (~95 Hz) did not vary with age or group. Intriguingly, log $i_{1/2}$ in 75 model rats was greater than that in controls or 50/10 model rats. Human adults with a history of ROP had lower-energy OPs than did the control adults, but infants with a history of ROP had higher-energy OPs than did the control infants F_{peak} was lower (~120 Hz) in infants than in adults (~130 Hz). ROP did not affect log $i_{1/2}$ in humans.

Conclusions—Differences between OPs in healthy rats and healthy humans were substantial, suggesting that OPs in rat models of ROP are unlikely to provide insight into the effects of ROP on human OPs. Indeed, neither ROP model studied showed a pattern of effects similar to that in human ROP.

The electroretinogram (ERG) is the only objective, noninvasive method available for determining the function of photoreceptors and other neural cells in the retina. The ERG recorded at the cornea of the dark-adapted vertebrate eye in response to a high-intensity flash includes two principle components: an initial negative deflection, the a-wave, and a subsequent positive deflection, the b-wave. The a-wave originates mainly in the collapse of the circulating current of the photo-receptors; the b-wave originates mainly in the onset of a radial current circulating around depolarizing bipolar cells.[1] Superimposed on the leading edge of the b-wave is a series of rhythmic, low-amplitude potentials called the oscillatory potentials (OPs).[2,3]

The OPs represent neural activity distinct from that of the a-and b-waves. Early OPs have been associated with photoreceptors and bipolar cells of the distal retina and late OPs with amacrine

Corresponding author: Anne B. Fulton, Department of Ophthalmology, Fegan 4, Children's Hospital, Boston, MA 02115; anne.fulton@childrens.harvard.edu.

Disclosure: **J.D. Akula**, None; **J.A. Mocko**, None; **A. Moskowitz**, None; **R.M. Hansen**, None; **A.B. Fulton**, None

and ganglion cells of the proximal retina.[4–8] However, possibly excepting the first OP which originates in the photoreceptors,[9,10] the OPs can be well modeled as one complex.[9–11] Thus, a neuron that spans the retinal layers and registers the activity of many classes of cells, such as the interplexiform cell, may be important in the generation of the OPs.[2,12,13] The amplitude and timing of the OP wavelets can be measured and studied individually or in sum. Alternatively, the OPs can be evaluated in the frequency domain by discreet Fourier transform (DFT) of the record. The DFT technique is especially advantageous when the signal-to-noise ratio is low.

The OPs are known to be affected in ocular conditions in which abnormal retinal blood vessels are the primary clinical sign, such as diabetic retinopathy,[14] glaucoma,[15,16] vascular occlusion,[17] and the developmental disorder retinopathy of prematurity (ROP).[18] Rat models of all these diseases have been reported.[19–28] These ailments have in common oxidative challenge to the inner retina.

In ERG studies of patients with a history of ROP, significant abnormalities in the a- and b-waves are found to persist into adulthood.[18,29,30] Similarly, ERG studies of rat models of ROP, created by exposing infant rats to periods of relatively high and low oxygen during the first weeks after birth, reveal deficits in a- and b-wave parameters similar to those found in the human condition.[13,27,28,31–33] Because the OPs can measure retinal sensitivity in ways not specified by the a- and b-waves, they may provide additional insight into disease processes in the inner neural retina. Whereas reports indicate that the OPs are diminished in rat ROP,[13,33] a comparison of the OPs in ROP rats and in human patients with ROP has not previously been undertaken. In this study, the OPs in two rat models of ROP and in human subjects with a history of ROP were characterized. Major differences in the effects of ROP on the OPs were found between the two species.

Methods

Rat Studies

Subjects—Thirty-six Sprague-Dawley albino rats (Charles River Laboratories, Inc., Worcester, MA) from 10 litters were studied. The light cycle was 12 hours dark and 12 hours light (50–100 lux). Care was taken to minimize the effects of mother and birth order. Pups were weaned at postnatal day (P)25. All tests were performed in all subjects at P20 ± 1, P30 ± 1, and P60 ± 1. Twelve rats were exposed to 75% oxygen from P7 to P14 (the 75 model). Twelve other rats were exposed to alternating 24 hour periods of 50% and 10% oxygen from P0 (the day of birth) to P14 (the 50/10 model). The two models produce a range of effects on the retinal vasculature and on the neural retina, as observed in the broad scope of human ROP.[28] The remaining 12 rats were reared in room air as controls. The a- and b-wave responses and the morphology of the retinal vasculature in these rats have been previously described.[28] At P20, the a- and b-waves of the ROP rats (75 and 50/10 models) were markedly attenuated.[27,28] All procedures in this study were approved by the Animal Care and Use Committee at Children's Hospital Boston and were performed in accordance with the ARVO Statement for the Use of Animals in Ophthalmic and Vision Research.

Procedures

Electroretinography: Dark-adapted ERGs were recorded at the cornea of the anesthetized rat by previously reported techniques.[28] The stimuli were brief (<1 ms), white flashes delivered through a 41-cm integrating sphere. The pupil was dilated with cyclopentolate/phenylephrine (Cyclomydril; Alcon, Fort Worth, TX). Stimulus intensity was controlled by calibrated neutral-density filters (Wratten; Eastman-Kodak, Rochester, NY). The unattenuated flash, measured at the position of the rat's eye using an integrating radiometer (S350; United Detector

Technology, Orlando, FL) produced ~40,000 $\mu W \cdot cm^{-2}$ at the cornea. This flash was calculated to elicit ~135,000 photoisomerizations of rhodopsin per rod (R*) in the adult control rat.[27,34] Flashes of doubling intensity (0.3-log-unit steps) ranging from ~6.3 R* to ~65,000 R* were presented. Half of the subjects in each group were not tested at flash intensities between ~270 R* and ~2100 R* to abbreviate recording time. Each stimulus was delivered at an interval that did not attenuate subsequent response amplitudes, 2 seconds for the dimmest and more than 2 minutes for the brightest. Nearly all records were single, unaveraged responses. Responses were amplified (×1000; 1–1000 Hz), digitized (2 kHz), and stored for off-line analysis (UTAS-E 2000, LKC Inc., Gaithersburg, MD).

Measurement of the Oscillatory Potentials: Figure 1 demonstrates the extraction of the OPs from an intact ERG. To mitigate the effects of a-wave contamination on the early OPs,[8–10,13,38,39] we fitted a mathematical model of the activation of phototransduction,[35–37] P3, to the leading edge of the a-wave and digitally subtracted the result from each trace. We digitally filtered the difference, P2, a putatively pure postreceptoral response, by using a second-order Butterworth filter[40] (MatLab; The MathWorks) with band-pass 60 to 235 Hz.[13]

The amplitude (in microvolts) and implicit time (in milliseconds) of the troughs and peaks in the filtered response were determined. For each OP (OP2, -3, -4, and -5), amplitude was defined as the difference between the peak and the trough immediately preceding it. Implicit time was defined as the time from stimulus onset to the peak. Despite the subtraction of P3, OP1 was occasionally visible but was not measured. The interpeak interval, *IPI* (in milliseconds), was defined as the time between adjacent OP peaks (OP2–3, OP3–4, OP4–5); mean *IPI* is a measure of periodicity.[39] For each trace, summed OP amplitude (*SOPA*) and summed OP implicit time (*SOPIT*) were used to characterize the OP response.

The OPs were also evaluated in the frequency domain. The first 256 samples (128 ms) of each record were subjected to a fast Fourier transform (radix-2 FFT algorithm; MATLAB; The MathWorks) to produce a power spectrum. Power in the frequency domain increases as the square of response amplitude in the time domain. However, the output of the FFT varies with the number of samples. To calibrate the output of the FFT, sine waves of fixed amplitude and an integer number of cycles per sample-set were subjected to the algorithm. These produced a single spike at the selected frequency that could be calibrated.[41] It was found that the equation

$$P(P', s) = \left(2 \cdot \frac{\sqrt{P'}}{\sqrt{s}}\right)^2 \quad (1)$$

properly calibrated OP power at each frequency, P (μV^2), from the radix-2 FFT power spectrum values, P', and the number of samples used in the FFT, s. Though the resistance in the recording circuit is unspecified, P is linearly proportional to OP power in Watts.

For responses with components at frequencies that do not result in an integer number of cycles in the measurement window, overspill occurs.[41] Thus, to characterize the OPs in the frequency domain, the calibrated data were fit by a Gaussian[10] of the form:

$$P(F) = \exp\left[-\frac{1}{2} \cdot \left(\frac{F - F_{peak}}{S}\right)^2\right] \cdot P_{peak}, \quad (2)$$

where P is the power in the response at frequency F (Hz), F_{peak} (Hz) is the frequency at the peak of the Gaussian, S (Hz) is a measure of the width of the distribution, and P_{peak} is the power at F_{peak}. F_{peak} is the dominant frequency of the OPs and is related to periodicity. The area under the Gaussian, E ($\mu V^2 \cdot s^{-1}$), was calculated by integrating equation 2, such that

$$E = P_{\text{peak}} \cdot S \cdot \sqrt{2\pi} \tag{3}$$

where E indicates the energy (proportional to joules) in the OPs and is related to the square of the summed OP amplitude, *SOPA*. To minimize any residual line-noise (60 Hz), observations in the frequency range of approximately 50 to 70 Hz were excluded from the fits.

Preliminary inspection of the data indicated that the relationship of OP energy and stimulus intensity was asymptotic. For each rat at each age, E was normalized to its maximum observed value (E_{max}), and the equation

$$\frac{E(i)}{E_{\text{max}}} = \frac{i^n}{i^n + i_{1/2}{}^n} \tag{4}$$

fit to OP power; both $i_{1/2}$ and n were free to vary. In this equation, i is the stimulus intensity (R*) and $i_{1/2}$ is the intensity of the stimulus that produces OPs with half-maximum energy. Although $1/i_{1/2}$ is a measure of OP sensitivity, it is analytically convenient to define the sensitivity of the OPs as log $i_{1/2}$.

Statistical Analyses—OP time domain parameters (*SOPA*, *SOPIT*, mean *IPI*) and frequency domain parameters (E, F_{peak}, log $i_{1/2}$) were evaluated by respective repeated-measures analyses of variance (ANOVA) with the factors age (P20, P30, P60), group (control, 75 model, 50/10 model), and intensity. Two intensities were selected for analysis because not all subjects were tested at all intensities. The lower intensity produced ~65 R*, too dim to activate cones but sufficient to saturate the rod-driven b-wave; the higher intensity produced ~8500 R*, sufficient to elicit a saturating a-wave and a saturating rod+cone b-wave.[42] Post hoc analyses were performed with the Tukey honestly significant difference (q) statistical test. The Pearson product moment correlation ($r2$) was used to evaluate the strength of the relationship between OP parameters and previously reported[28] parameters of the a- and b-waves. The significance level (α) for all tests was $P < 0.05$.

Human Studies

Subjects—Ninety-one subjects participated: 51 infants and 40 adults. All subjects fell into one of four groups: (1) term-born infants in good general health ($n = 38$; age, 63–78 days at test); (2) ROP infants, infants with a history of ROP ($n = 13$; age 60–82 days postterm at test); (3) adult controls with good visual acuity and no high refractive errors ($n = 26$; age, 8–52 years at test); or (4) ROP adults, adults with a history of ROP ($n = 14$; age, 7–23 years at test). ROP was diagnosed in the neonatal intensive care unit by a pediatric ophthalmologist expert in ROP. In each ROP subject, the ROP was mild and resolved spontaneously. Rod a- and b-wave responses have been reported previously for nearly all subjects in this study.[30,43] In normal subjects, all a- and b-wave response parameters are mature by age 6 months.[43] This study was approved by the Committee on Clinical Investigation at Children's Hospital Boston and adhered to the tenets of the World Medical Association Declaration of Helsinki. Written informed consent was obtained from all subjects or their parents.

Procedures

Electroretinography: Dark-adapted ERGs were recorded from one eye of each subject, using previously described techniques.[39] The pupil was dilated (Cyclogyl 1%; Alcon, Fort Worth, TX). Brief (<1 ms), full-field blue flashes (Wratten 47B; $\lambda < 510$ nm) were presented (model 600 VR, series 2100; Novatron, Dallas, TX) in an integrating sphere. Responses were differentially amplified (×1000; 1–1000 Hz), digitized (2.56 kHz), and stored (Compact 4 system; Nicolet Biomedical, Madison, WI).

Retinal illuminance varies directly with pupil diameter and the transmissivity of the ocular media and inversely with the square of the posterior–nodal distance.[44] Though the density of the ocular media is significantly lower in 10-week-old infants than in adults,[45] when pupil area, posterior–nodal distance, and ocular media density are taken into account, a given intensity flash produces approximately equal retinal illuminance in young infants and adults.[46,47] Based on the work of Kraft et al.,[48] Hansen and Fulton[49] estimated that the difference in rate of photoisomerization in adults and 10 week-old infants was only ~0.1 log unit. The unattenuated flash produced ~3.0 log scot td · s, or ~8500 R*. Neutral density filters were used to present stimuli of doubling intensity over an ~2.1-log-unit range (~65 to ~8500 R*). Stimuli were delivered at a rate that did not attenuate subsequent response amplitudes.

Measurement of the Oscillatory Potentials: Similar to the method for the rat ERGs, for each human response, P3 was fitted to the leading edge of the a-wave and digitally subtracted from the record. To demonstrate the OPs, the resultant P2 was digitally filtered with a second-order Butterworth filter with the ISCEV (International Society for Clinical Electrophysiology of Vision)-recommended bandpass of 75 to 300 Hz.[50] In the time domain, the amplitudes and implicit times of OP2, -3, -4, and -5 were measured and the OP2–3, OP3–4, and OP4–5 interpeak intervals calculated. The first 128 samples (50 ms) of each record were then subjected to FFT (MatLab; The MathWorks). This duration is sufficient to capture all OPs.[39] The resultant frequency domain data were fitted by a Gaussian, and the OP frequency, F_{peak} (equation 2); energy, E (equation 3); and sensitivity, log $i_{1/2}$ (equation 4) were calculated.

Statistical Analyses—OP frequency domain parameters (E, F_{peak}, log$i_{1/2}$) were evaluated by respective repeated measures ANOVAs, with the factors age (infant, adult), clinical history (ROP, no ROP), and intensity (65–8500 R*). Post hoc analyses were performed with the Tukey honestly significant difference (q) statistical test. The significance level (α) for all tests was $P < 0.05$.

Results

Rat Studies

For each group (control, 75 model, 50/10 model) and intensity (65 R*, 8500 R*) mean OP2, -3, -4, and -5 trough and peak amplitudes and implicit times were calculated. Figure 2 summarizes the time domain analysis in P20 rats. Time-domain OP parameter values at each age and results of ANOVA on these data are presented in Table 1. Amplitudes were larger and implicit times were shorter for OP responses to the 8500 R* stimulus than to the 65 R* stimulus. At the higher intensity, the OP amplitudes were larger in the control rats than in either the 50/10 model or the 75 model rats; at the lower (scotopic) intensity, the 50/10 model rats' OP amplitudes were markedly attenuated, but 75 model rats' OPs differed little from controls'. ROP did not affect *SOPIT*, but 50/10 model rats' *IPI*s were significantly longer than *IPI*s in either the control or 75 model groups.

Figure 3 shows the OPs of P20 rats transformed into the frequency domain by DFT. In the left panels, mean OP power for control, 75 model, and 50/10 model rats is plotted against frequency and flash intensity. In the right panels, fits of equation 1 to the 65 R* and 8500 R* flashes are shown. Frequency domain OP parameter values at each age and results of ANOVAs on these data are presented in Table 2. OP power at F_{peak}, P_{peak} (equation 2), and OP energy, E (equation 3), the area under the curve, increased with stimulus intensity. E and F_{peak} were significantly lower in the 50/10 model rats than in the controls. The 75 model rats did not differ significantly from controls in either parameter.

Figure 4 plots the change in the time domain parameters *SOPA* and *IPI*, and in the frequency domain parameters E and F_{peak}, as a percent of control at each test age for the 8500 R* flash.

The group × age interaction was not significant for either *SOPA* (Table 1) or *E* (Table 2), indicating that the OPs in ROP rats remained below normal across ages. Periodicity, indicated by *IPI* and F_{peak}, became relatively shorter with age in ROP rats.

OP sensitivity, indicated by the parameter log $i_{1/2}$ (equation 4; Fig. 5A), differed significantly from normal in ROP rats (Table 2). Surprising, however, was the direction of the abnormality. As indicated in Figures 5B and 5C, 75 model rats at all test ages were significantly more sensitive than both controls and 50/10 model rats. At P20, 50/10 model rats were slightly (but not significantly) less sensitive than controls, but at P30 and P60 were slightly more sensitive than controls. Log $i_{1/2}$ was the only parameter for which 75 model rats differed significantly from controls (Tukey HSD test).

Across groups, at each test age (P20, P30, and P60) both *SOPA* and *E* correlated significantly with the previously reported saturating a- and b-wave amplitudes (Rm_{P3} and *Vm* parameters) in these same rats.[28] The sensitivity of the OPs (log $i_{1/2}$), however, did not correlate with the sensitivities of either the a- or b-waves (*S* and log σ parameters).[28] The tortuosity of the retinal vasculature (IC_A parameter) did not correlate significantly with OP amplitude, energy, or sensitivity.[28]

Human Studies

Figure 6A demonstrates the derivation of the OPs in an adult control subject. The OPs in human adults were comparable in amplitude to those in control rats. However, as previously reported, the amplitudes of the OPs in the healthy, term-born infants were small (median, <5 μV), similar to root mean squared noise (~3 μV). In the frequency domain, however, a small peak at the frequency expected from the interpeak interval was always found, and thus the DFT proved a superior OP analysis technique to time domain trough and peak measurements in these data with low signal.

Data from the adult controls, ROP adults, term-born infants, and ROP infants groups, transformed into the frequency domain, are presented in Figure 6B. Frequency domain OP parameters at each age and results of ANOVAs on these data are presented in Table 3. In the frequency domain data, the spectra in both control and ROP adults were bimodally distributed with peaks at ~100 and ~140 Hz at 8500 R*. The higher frequency peak agreed well with interpeak interval (~7 ms). Accordingly, equation 3 was fit to the higher-frequency peak. In contrast, spectra in both term-born and ROP infants show a single peak at ~127 and ~112 Hz, respectively. In both adults and infants, with and without a history of ROP, the dominant OP frequency, F_{peak}, increased with increasing flash intensity (Table 3). The OPs in ROP adults had less energy than those in adult controls. Surprisingly, OPs in ROP infants had significantly more energy than the OPs in age-matched, term-born infants.

Figure 7 plots the frequency domain parameters in ROP infants and ROP adults as a proportion of the values in term-born infants and adult controls, respectively. The energy in the OPs, *E*, was significantly higher (>1 log unit) in ROP than in term-born infants but was significantly lower (~0.3 log units) in ROP than in control adults. Overall, OP energy was significantly higher in adults than in infants. There was no significant difference in the dominant frequency of the OPs, F_{peak}, between ROP and healthy subjects in either infancy or adulthood. ROP did not affect the sensitivity of the OPs (log $i_{1/2}$) in either infants or adults. Sensitivity was, however, significantly greater in adult than in infant subjects.

Discussion

The OPs were affected by ROP in both species, rat and human, but in different ways. In the rats, the OPs in the 50/10 model were slower, smaller, and lower energy than in controls and

did not improve with age. Sensitivity did not differ from controls in 50/10 model rats but was the only parameter that differed from controls in 75 model rats. Intriguingly, the sensitivity of the OPs was greater in 75 model rats than in controls or in 50/10 model rats. In the human subjects, on the other hand, only OP energy was abnormal. The direction of the abnormality changed with age. The energy in the ROP infants' OPs was dramatically higher, about a log unit on average, than in the term-born infants', but only half as high in ROP adults as in adult controls. The significantly greater deficits in both the ROP rat models' OP amplitude (*SOPA*, Table 1) and energy (*E*, Table 2) at higher stimulus intensities may reflect a greater deficit in the cone pathway. In the human subjects, the history × intensity interaction for *E* (Table 3) was not significant.

Why, with the exception of OP sensitivity, were the rat OPs less affected by ROP in the 75 model than in the 50/10 model? Presumably, fully differentiated cell types are less susceptible to oxygen perturbations than those still undergoing extensive developmental alterations.[51] The 50/10 induction begins at P0, when the retina is extremely immature. Ganglion cells are identifiable, but the remainder of the retina is a single layer of neuroblastic cells.[52,53] Thus, the 50/10 exposure may interfere with the differentiation and development of every class of neuron in the retina. The 75 model induction begins later, at P7, after all cell types are differentiated and the developmental elongation of photoreceptor outer segments has begun; however, extensive refinements to neural circuitry are still underway.[54] Thus, three possible (not mutually exclusive) explanations for the robust OPs in the 75 model are: (1) By P7, the cells that generate the OPs are relatively insensitive to retinal hyperoxia (2); the cells that generate the OPs are more susceptible to hypoxia than hyperoxia; and (3) the alternation between hyperoxia and hypoxia is more damaging to the OP generator(s) than is sustained hyperoxia. In addition, attenuation of inhibitory retinal circuitry results in enhanced OPs.[55] There is some evidence that excitatory pathways to retinal ganglion cells in the rat are present, if not mature, by P5, but inhibitory pathways are not.[56] Thus, it is also possible that the observed enhanced sensitivity of the OPs in the 75 model is due to selective disruption of later-developing inhibitory synaptic connections.

Vascular endothelial growth factor (VEGF) is induced by hypoxia and drives developmental vascularization of the retina as well as the pathologic retinal vascularization characteristic of ROP.[57–60] In addition, amacrine cell progenitors are directed to their cell fate by a number of cues, including activation of the VEGF receptor flk-1.[61] In murine retina, amacrine cells, including the interplexiform cell, are still differentiating at P0 but are fully differentiated at P7.[54] Thus, the number and type of postreceptoral cells may be at least partially dependent on the status of retinal oxygenation. We found that the tortuous vasculature characteristic of ROP remodeled (that is, became more normal) remarkably after P20 in the 50/10 model rats, but only slightly in the 75 model rats.[28] Since the OPs are susceptible to disturbances of retinal circulation,[62] their function may be related to the severity of retinal vascular abnormality in ROP. However, the data did little to affirm this. There was no significant correlation between vascular abnormality and *E* or log $i_{1/2}$ at P20, P30, or P60.

As in the ROP rats, the adult human subjects with a history of ROP had lower energy in their OPs than the adult controls. However, the ROP infants' OPs contained more energy than those in term-born infants. Developing retinal circuitry must underpin the maturation of the OPs. Both infant groups were age-matched postterm, but the ROP infants had, on average, been using their eyes for more than twice the duration of the term-born infants (~3 extra months). If use of vision promotes the development of the inner retinal circuitry that generate the OPs, then the ROP infants' additional early visual experience may have more than offset the negative effects of mild ROP[30] and resulted in the observed increase in their OP energy. Evidence from the sweep visual evoked potential indicated that prematurely born infants, both with[63] and without[64] ROP, have better acuity than term-born infants, though behavioral acuity tests at ~6

months found that the advantage has vanished if not reversed.[65] The visual experience of the rats did not vary with group.

The shapes of the rat and human OP power spectra also differed. First, the dominant frequency of the OPs (F_{peak}) was much higher in the human subjects than in the rats (~130 Hz vs. ~95 Hz at 8500 R*) across all ages and groups. Second, though recorded and processed nearly analogously, the rats' OP power spectrum was unimodally distributed at all ages, whereas, in agreement with previous reports,[9,10] the adult humans' OP power spectrum was bimodal. The faster peak matched the interpeak interval (~7 ms). The origin of the lower-frequency peak remains to be specified. This second, slower peak, was not present in the human infants' power spectra.

The DFT permitted reliable evaluation of the OPs in the term-born human infants, even though the signal-to-noise ratio in the time domain was very low. Although use of an analog (Butterworth) filter introduces a slight phase shift,[40] the filter has the benefit of removing the b-wave ramp-artifact[41] (low-frequency, high-amplitude noise) from the record. The use of a Gaussian fit to the power spectrum is advised because periodicity and sampling rate both affect OP power, but the area under the curve (E in equation 3) remains constant. The peak of the Gaussian (F_{peak} in equation 2) also provides an unbiased measure of the dominant frequency of the OPs that is less susceptible to artifactual spikes in the data.

That there were marked interspecies differences between the OP power spectra in healthy rats and humans implies that the neural underpinnings of the OPs may be distinct in the two species. Therefore, it is not surprising that the pattern of OP responses in the 75 and 50/10 models of ROP did not resemble the pattern of OP responses in human ROP. Until the origins of the OPs are better specified, it will be difficult to interpret the physiological significance of unexpected observations such as the heightened sensitivity of the OPs in 75 model ROP rats or the increased OP energy in infants with a history of ROP.

Acknowledgements

The authors thank Professor Michael Bach for aid in understanding the behavior of the DFT and an anonymous reviewer for contributions to the Discussion.

Supported by National Eye Institute Grant R01 EY10597 and by grants from the Knights Templar Eye Research Fund, the Fight for Sight, the March of Dimes Birth Defects Foundation, the Pearle Vision Foundation, and the Massachusetts Lions Eye Research Fund.

References

1. Pugh, EN., Jr; Falsini, B.; Lyubarsky, AL. The origins of the major rod-and cone- driven components of the rodent electroretinogram and the effect of age and light-rearing history on the magnitude of these components. In: Williams, TP.; Thistle, AB., editors. Photostasis and Related Phenomena. New York: Plenum Press; 1998. p. 93-128.
2. Wachtmeister L. Oscillatory potentials in the retina: what do they reveal. Prog Retin Eye Res 1998;17:485–521. [PubMed: 9777648]
3. Wachtmeister L. Some aspects of the oscillatory response of the retina. Prog Brain Res 2001;131:465–474. [PubMed: 11420963]
4. Brown KT. The electroretinogram: its components and their origins. Vision Res 1968;8:633–677. [PubMed: 4978009]
5. Ogden TE. The oscillatory waves of the primate electroretinogram. Vision Res 1973;13:1059–1074. [PubMed: 4197416]
6. Rangaswamy NV, Hood DC, Frishman LJ. Regional variations in local contributions to the primate photopic flash ERG: revealed using the slow-sequence mfERG. Invest Ophthalmol Vis Sci 2003;44:3233–3247. [PubMed: 12824276]

7. Moller A, Eysteinsson T. Modulation of the components of the rat dark-adapted electroretinogram by the three subtypes of GABA receptors. Vis Neurosci 2003;20:535–542. [PubMed: 14977332]
8. Dong CJ, Agey P, Hare WA. Origins of the electroretinogram oscillatory potentials in the rabbit retina. Vis Neurosci 2004;21:533–543. [PubMed: 15579219]
9. Van der Torren K, Groeneweg G, van Lith G. Measuring oscillatory potentials: Fourier analysis. Doc Ophthalmol 1988;69:153–159. [PubMed: 3168718]
10. Bui BV, Armitage JA, Vingrys AJ. Extraction and modelling of oscillatory potentials. Doc Ophthalmol 2002;104:17–36. [PubMed: 11949806]
11. Derr PH, Meyer AU, Haupt EJ, Brigell MG. Extraction and modeling of the oscillatory potential: signal conditioning to obtain minimally corrupted oscillatory potentials. Doc Ophthalmol 2002;104:37–55. [PubMed: 11949807]
12. Heynen H, Wachtmeister L, van Norren D. Origin of the oscillatory potentials in the primate retina. Vision Res 1985;25:1365–1373. [PubMed: 4090272]
13. Liu K, Akula JD, Hansen RM, Moskowitz A, Kleinman MS, Fulton AB. Development of the electroretinographic oscillatory potentials in normal and ROP rats. Invest Ophthalmol Vis Sci 2006;47:5447–5452. [PubMed: 17122135]
14. Yonemura D, Aoki T, Tsuzuki K. Electroretinogram in diabetic retinopathy. Arch Ophthalmol 1962;68:19–24. [PubMed: 14009176]
15. Holopigian K, Greenstein VC, Seiple W, Hood DC, Ritch R. Electrophysiologic assessment of photoreceptor function in patients with primary open-angle glaucoma. J Glaucoma 2000;9:163–168. [PubMed: 10782626]
16. Ferreri G, Buceti R, Ferreri FM, Roszkowska AM. Postural modifications of the oscillatory potentials of the electroretinogram in primary open-angle glaucoma. Ophthalmologica 2002;216:22–26. [PubMed: 11901284]
17. Hara A, Miura M. Decreased inner retinal activity in branch retinal vein occlusion. Doc Ophthalmol 1994;88:39–47. [PubMed: 7743911]
18. Fulton AB, Hansen RM. Photoreceptor function in infants and children with a history of mild retinopathy of prematurity. J Opt Soc Am A Opt Image Sci Vis 1996;13:566–571. [PubMed: 8627413]
19. Penn JS, Tolman BL, Henry MM. Oxygen-induced retinopathy in the rat: relationship of retinal nonperfusion to subsequent neovascularization. Invest Ophthalmol Vis Sci 1994;35:3429–3435. [PubMed: 8056518]
20. Penn JS, Henry MM, Wall PT, Tolman BL. The range of PaO_2 variation determines the severity of oxygen-induced retinopathy in newborn rats. Invest Ophthalmol Vis Sci 1995;36:2063–2070. [PubMed: 7657545]
21. Morrison JC, Moore CG, Deppmeier LM, Gold BG, Meshul CK, Johnson EC. A rat model of chronic pressure-induced optic nerve damage. Exp Eye Res 1997;64:85–96. [PubMed: 9093024]
22. Sawada A, Neufeld AH. Confirmation of the rat model of chronic, moderately elevated intraocular pressure. Exp Eye Res 1999;69:525–531. [PubMed: 10548472]
23. Daugeliene L, Niwa M, Hara A, et al. Transient ischemic injury in the rat retina caused by thrombotic occlusion-thrombolytic reperfusion. Invest Ophthalmol Vis Sci 2000;41:2743–2747. [PubMed: 10937592]
24. Cunningham S, McColm JR, Wade J, Sedowofia K, McIntosh N, Fleck B. A novel model of retinopathy of prematurity simulating preterm oxygen variability in the rat. Invest Ophthalmol Vis Sci 2000;41:4275–4280. [PubMed: 11095626]
25. Bayer AU, Danias J, Brodie S, et al. Electroretinographic abnormalities in a rat glaucoma model with chronic elevated intraocular pressure. Exp Eye Res 2001;72:667–677. [PubMed: 11384155]
26. Hancock HA, Kraft TW. Oscillatory potential analysis and ERGs of normal and diabetic rats. Invest Ophthalmol Vis Sci 2004;45:1002–1008. [PubMed: 14985323]
27. Liu K, Akula JD, Falk C, Hansen RM, Fulton AB. The retinal vasculature and function of the neural retina in a rat model of retinopathy of prematurity. Invest Ophthalmol Vis Sci 2006;47:2639–2647. [PubMed: 16723481]

28. Akula JD, Hansen RM, Martinez-Perez ME, Fulton AB. Rod photo-receptor function predicts blood vessel abnormality in retinopathy of prematurity. Invest Ophthalmol Vis Sci 2007;48:4351–4359. [PubMed: 17724227]
29. Fulton AB, Hansen RM. Electroretinogram responses and refractive errors in patients with a history of retinopathy prematurity. Doc Ophthalmol 1995;91:87–100. [PubMed: 8813488]
30. Fulton AB, Hansen RM, Petersen RA, Vanderveen DK. The rod photoreceptors in retinopathy of prematurity: an electroretinographic study. Arch Ophthalmol 2001;119:499–505. [PubMed: 11296015]
31. Fulton AB, Reynaud X, Hansen RM, Lemere CA, Parker C, Williams TP. Rod photoreceptors in infant rats with a history of oxygen exposure. Invest Ophthalmol Vis Sci 1999;40:168–174. [PubMed: 9888440]
32. Dembinska O, Rojas LM, Varma DR, Chemtob S, Lachapelle P. Graded contribution of retinal maturation to the development of oxygen-induced retinopathy in rats. Invest Ophthalmol Vis Sci 2001;42:1111–1118. [PubMed: 11274093]
33. Dembinska O, Rojas LM, Chemtob S, Lachapelle P. Evidence for a brief period of enhanced oxygen susceptibility in the rat model of oxygen-induced retinopathy. Invest Ophthalmol Vis Sci 2002;43:2481–2490. [PubMed: 12091454]
34. Fulton AB, Hansen RM, Findl O. The development of the rod photoresponse from dark-adapted rats. Invest Ophthalmol Vis Sci 1995;36:1038–1045. [PubMed: 7730013]
35. Lamb TD, Pugh EN Jr. A quantitative account of the activation steps involved in phototransduction in amphibian photoreceptors. J Physiol 1992;449:719–758. [PubMed: 1326052]
36. Pugh EN Jr, Lamb TD. Amplification and kinetics of the activation steps in phototransduction. Biochim Biophys Acta 1993;1141:111–149. [PubMed: 8382952]
37. Hood DC, Birch DG. Rod phototransduction in retinitis pigmentosa: estimation and interpretation of parameters derived from the rod a-wave. Invest Ophthalmol Vis Sci 1994;35:2948–2961. [PubMed: 8206712]
38. Asi H, Leibu R, Perlman I. Frequency-domain analysis of the human corneal electroretinogram. Clin Vis Sci 1992;7:9–19.
39. Moskowitz A, Hansen RM, Fulton AB. ERG Oscillatory potentials in infants. Doc Ophthalmol 2005;110:265–270. [PubMed: 16328935]
40. Lei B, Yao G, Zhang K, Hofeldt KJ, Chang B. Study of rod- and cone-driven oscillatory potentials in mice. Invest Ophthalmol Vis Sci 2006;47:2732–2738. [PubMed: 16723493]
41. Bach M, Meigen T. Do's and don'ts in Fourier analysis of steady-state potentials. Doc Ophthalmol 1999;99:69–82. [PubMed: 10947010]
42. Akula JD, Lyubarsky AL, Naarendorp F. The sensitivity and spectral identity of the cones driving the b-wave of the rat electroretinogram. Vis Neurosci 2003;20:109–117. [PubMed: 12916733]
43. Fulton AB, Hansen RM. The development of scotopic sensitivity. Invest Ophthalmol Vis Sci 2000;41:1588–1596. [PubMed: 10798680]
44. Pugh, EN, Jr. Vision: physical and retinal physiology. In: Atkinson, RC., editor. Stevens' Handbook of Experimental Psychology. 2. New York: Wiley; 1988. p. 75-163.
45. Hansen RM, Fulton AB. Psychophysical estimates of ocular media density of human infants. Vision Res 1989;29:687–690. [PubMed: 2626826]
46. Brown AM, Dobson V, Maier J. Visual acuity of human infants at scotopic, mesopic and photopic luminances. Vision Res 1987;27:1845–1858. [PubMed: 3445474]
47. Hansen, RM.; Fulton, AB. Development of scotopic retinal sensitivity. In: Simons, K., editor. Early Visual Development, Normal and Abnormal. New York: Oxford University Press; 1993. p. 130-142.
48. Kraft TW, Schneeweis DM, Schnapf JL. Visual transduction in human rod photoreceptors. J Physiol 1993;464:747–765. [PubMed: 8229828]
49. Hansen RM, Fulton AB. Recovery of the rod photoresponse in infants. Invest Ophthalmol Vis Sci 2005;46:764–768. [PubMed: 15671311]
50. Marmor MF, Holder GE, Seeliger MW, Yamamoto S. Standard for clinical electroretinography (2004 update). Doc Ophthalmol 2004;108:107–114. [PubMed: 15455793]

51. Maslim J, Valter K, Egensperger R, Hollander H, Stone J. Tissue oxygen during a critical developmental period controls the death and survival of photoreceptors. Invest Ophthalmol Vis Sci 1997;38:1667–1677. [PubMed: 9286255]
52. Weidman TA, Kuwabara T. Development of the rat retina. Invest Ophthalmol 1969;8:60–69. [PubMed: 5763846]
53. Kuwabara T, Weidman TA. Development of the prenatal rat retina. Invest Ophthalmol 1974;13:725–739. [PubMed: 4412789]
54. Young RW. Cell differentiation in the retina of the mouse. Anat Rec 1985;212:199–205. [PubMed: 3842042]
55. McCall MA, Lukasiewicz PD, Gregg RG, Peachey NS. Elimination of the rho1 subunit abolishes GABA(C) receptor expression and alters visual processing in the mouse retina. J Neurosci 2002;22:4163–4174. [PubMed: 12019334]
56. Rorig B, Grantyn R. Glutamatergic and GABAergic synaptic currents in ganglion cells from isolated retinae of pigmented rats during postnatal development. Brain Res Dev Brain Res 1993;74:98–110.
57. Pierce EA, Avery RL, Foley ED, Aiello LP, Smith LE. Vascular endothelial growth factor/vascular permeability factor expression in a mouse model of retinal neovascularization. Proc Natl Acad Sci USA 1995;92:905–909. [PubMed: 7846076]
58. Provis JM, Leech J, Diaz CM, Penfold PL, Stone J, Keshet E. Development of the human retinal vasculature: cellular relations and VEGF expression. Exp Eye Res 1997;65:555–568. [PubMed: 9464188]
59. Aiello LP. Vascular endothelial growth factor and the eye: biochemical mechanisms of action and implications for novel therapies. Ophthalmic Res 1997;29:354–362. [PubMed: 9323726]
60. Gariano RF, Hu D, Helms J. Expression of angiogenesis-related genes during retinal development. Gene Expr Patterns 2006;6:187–192. [PubMed: 16330258]
61. Cepko CL, Austin CP, Yang X, Alexiades M, Ezzeddine D. Cell fate determination in the vertebrate retina. Proc Natl Acad Sci USA 1996;93:589–595. [PubMed: 8570600]
62. Speros P, Price J. Oscillatory potentials: history, techniques and potential use in the evaluation of disturbances of retinal circulation. Surv Ophthalmol 1981;25:237–252. [PubMed: 7010647]
63. Mirabella G, Kjaer PK, Norcia AM, Good WV, Madan A. Visual development in very low birth weight infants. Pediatr Res 2006;60:435–439. [PubMed: 16940247]
64. Norcia AM, Tyler CW, Piecuch R, Clyman R, Grobstein J. Visual acuity development in normal and abnormal preterm human infants. J Pediatr Ophthalmol Strabismus 1987;24:70–74. [PubMed: 3585654]
65. Spierer A, Royzman Z, Kuint J. Visual acuity in premature infants. Ophthalmologica 2004;218:397–401. [PubMed: 15564758]

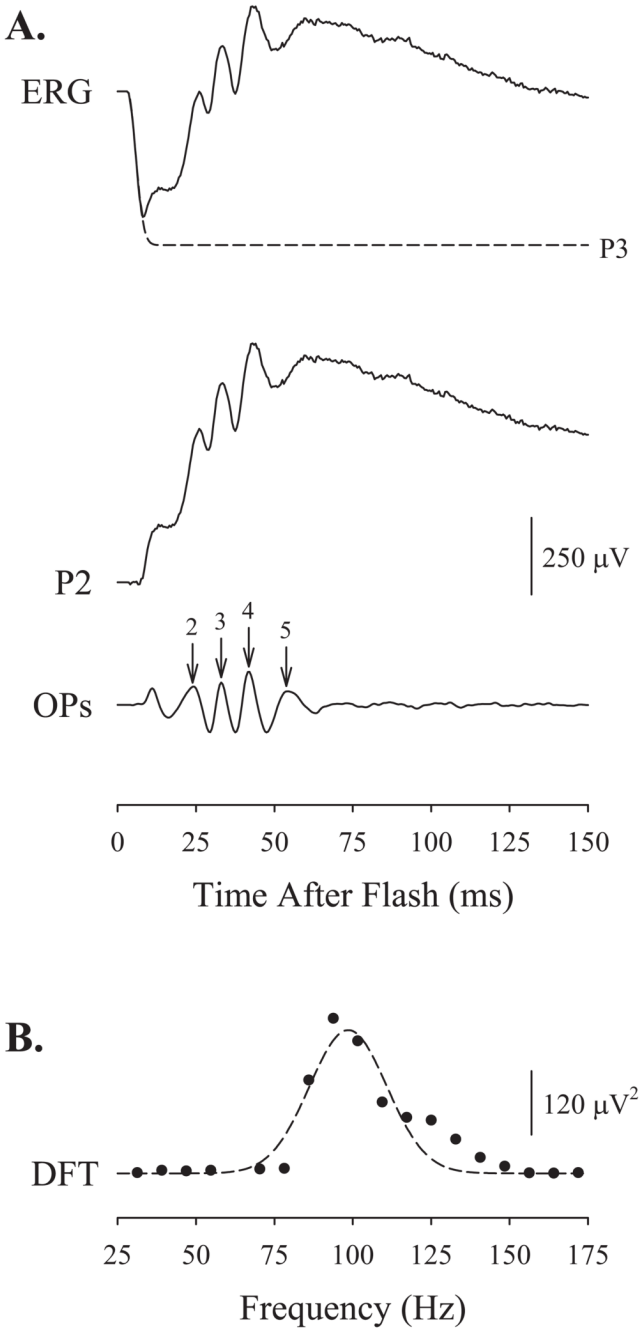

Figure 1.

Extraction of the electroretinographic oscillatory potentials (OPs). (**A**) An intact ERG elicited from a P20 control rat by a flash producing ~8500 photoisomerizations of rhodopsin per rod (R*). Fitted to the leading edge of the a-wave is a mathematical model of the activation of phototransduction, P3 (*dashed line*).[35–37] P3 is digitally subtracted from the trace to produce the putatively pure postreceptoral P2. The OPs are demonstrated by passing P2 through a second-order Butterworth filter with band-pass of 60 to 235 Hz. The amplitude of the OPs (numbered) is measured to the peak of the OP wavelet from the trough immediately preceding it. The implicit time of each OP is measured from stimulus onset to the peak. (**B**) The OPs are

transformed into the frequency domain by DFT of the filtered record. A Gaussian (equation 2) is fitted to the power spectrum (*dashed line*).

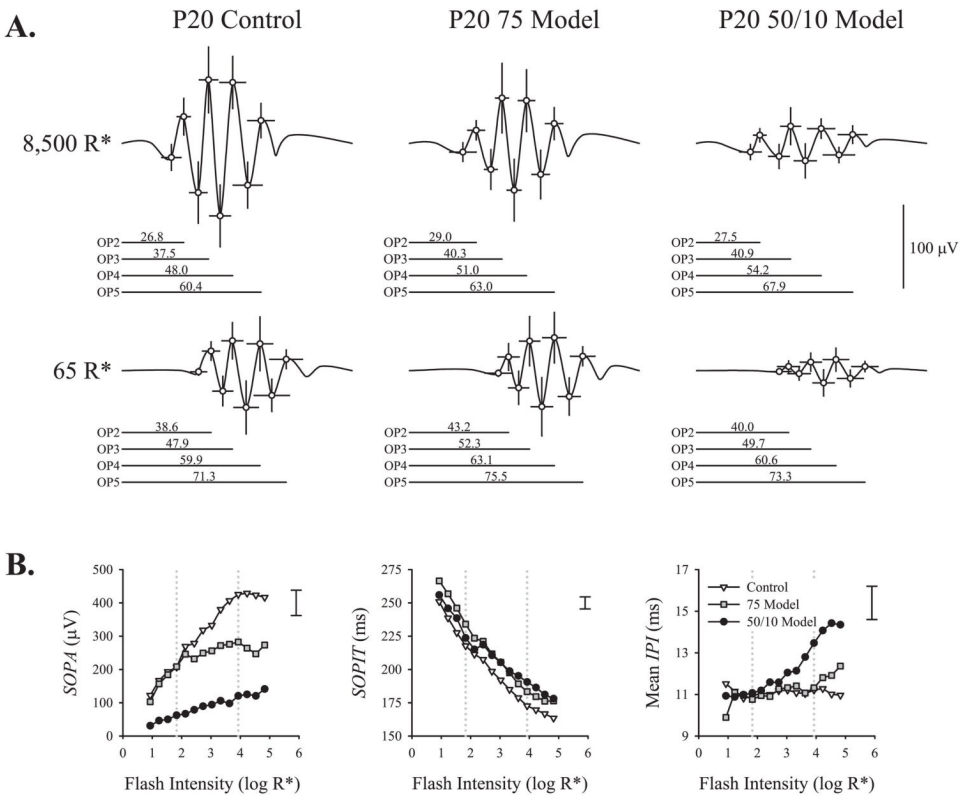

Figure 2.

Time domain analysis. (**A**) Mean (±SD) OP2, -3, -4, and -5 trough and peak amplitudes and implicit times plotted for P20 control, 75 model, and 50/10 model rats' responses to the 8500 R* and 65 R* stimuli. In this display, the points are connected with a spline curve (SigmaPlot 10; Systat Software, Inc., San Jose, CA) to simulate average OPs. The mean implicit time for each OP peak is indicated below each record. (**B**) Mean *SOPA*, mean *SOPIT*, and mean *IPI* (periodicity) are plotted as a function of flash intensity. *Dotted lines*: intensities shown in (**A**). Error bars at the *top right* of each panel indicate the average ± SEM across groups at 8500 R*. Error at other intensities was a similar proportion of the mean.

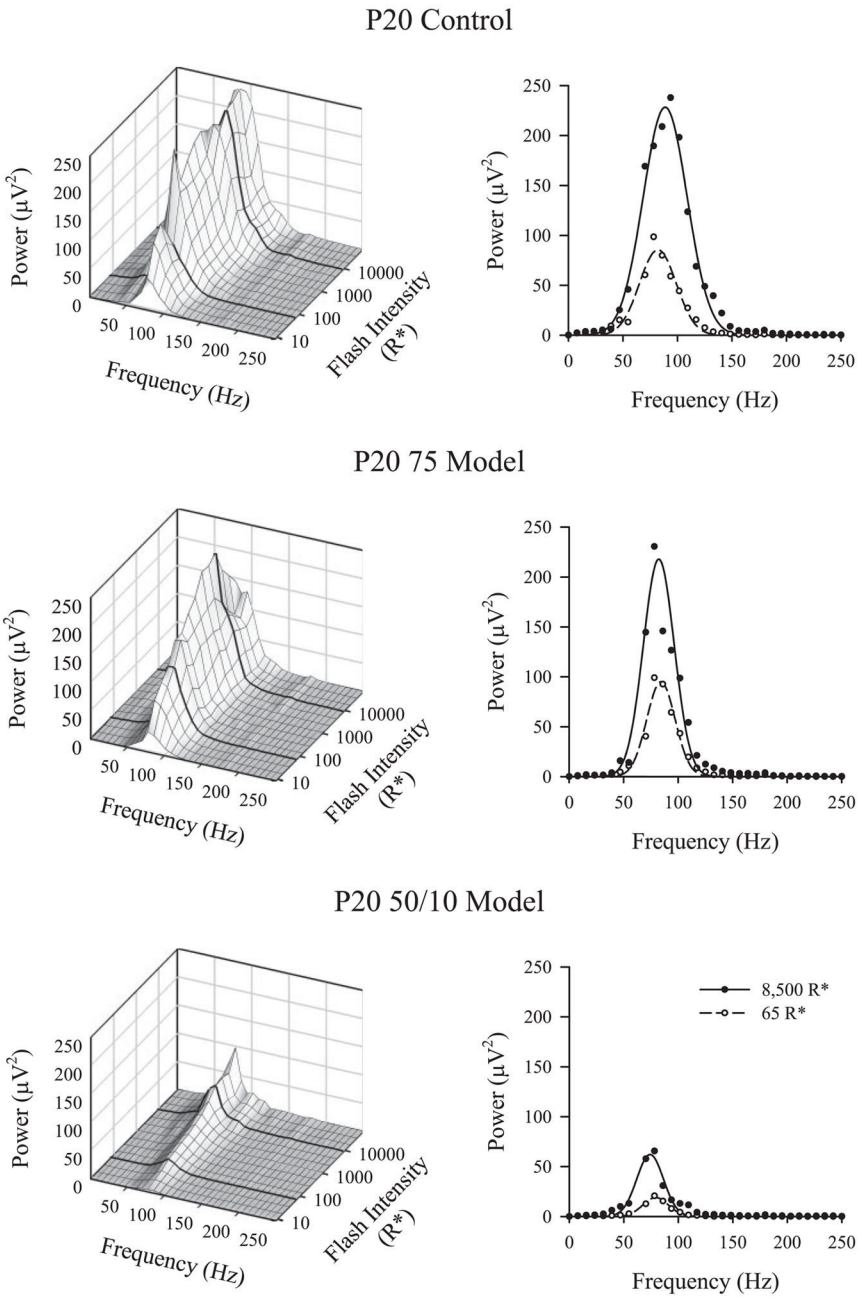

Figure 3.

Frequency domain analysis. *Left*: the mean OP power as a function of frequency and intensity for P20 control, 75 model, and 50/10 model rats. *Bold lines*: 8500 R* and 65 R* stimulus levels. *Right*: replot the frequency domain responses (*circles*) to these stimuli with fits of equation 2. The area under the curve (equation 3) indicates OP energy.

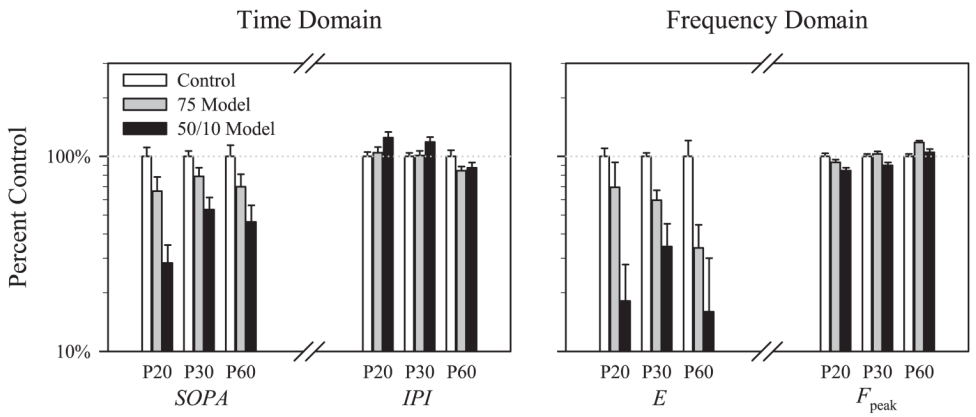

Figure 4.

The time domain parameters *SOPA* and *SOPIT* and frequency domain parameters OP energy (*E*) and dominant frequency (F_{peak}) plotted as a percentage of the control (+SEM) at each test age (P20, P30, and P60) for 75 model and 50/10 model rats. The control mean for each parameter is 100% (*dotted line*).

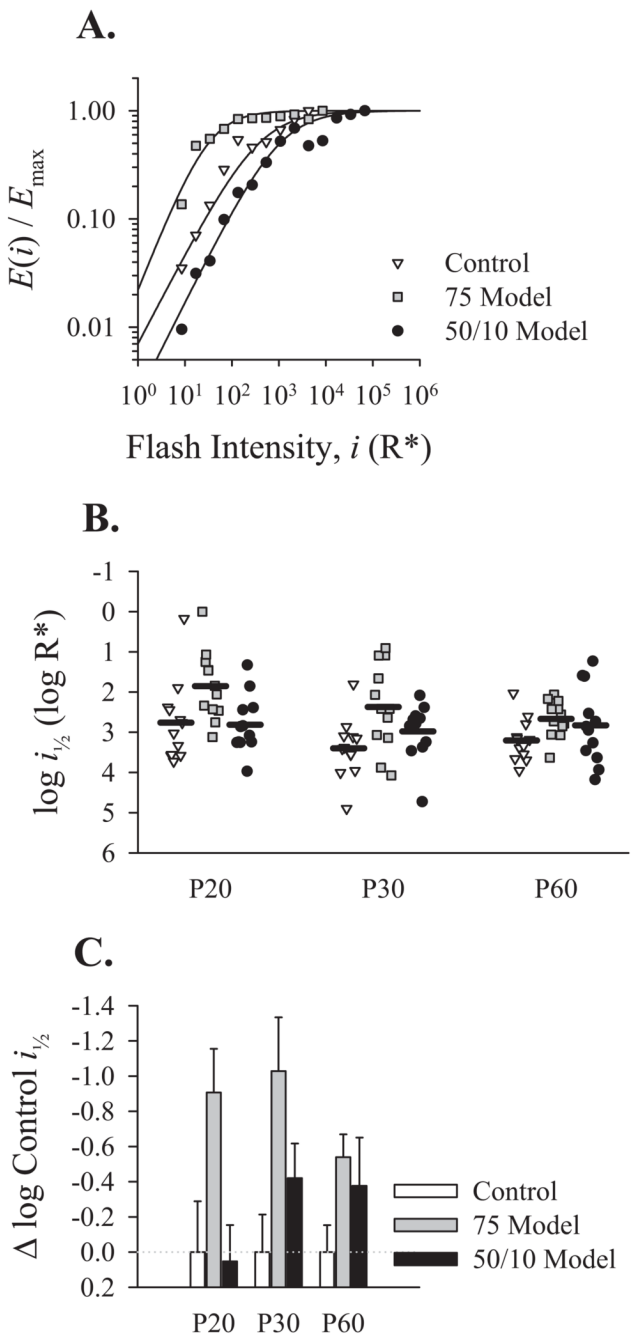

Figure 5.

The sensitivity of the OPs derived from OP energy (*E*). (**A**) For each rat at each age, OP energy at every intensity was divided by the maximum observed energy and fit by equation 4. Shown are representative energy versus intensity relationships for respective P20 control, 75 model, and 50/10 model rats. (**B**) The sensitivity of the OPs, indicated by the log of the intensity required to elicit a response with half-maximum OP energy, log $i_{1/2}$, plotted for each group at P20, P30, and P60. *Horizontal bars*: mean for each group at each age. (**C**) Mean OP sensitivity (from **B**) for 75 model and 50/10 model rats replotted as a proportion of the control mean (+SEM) at each test age. The control mean for each parameter is 0.0 (*dotted line*).

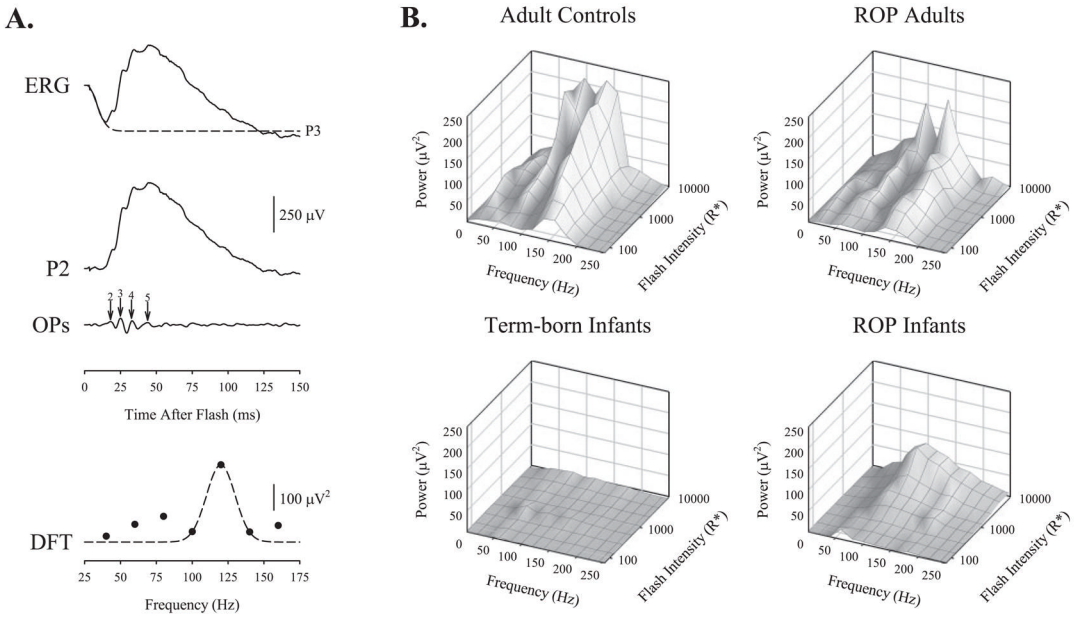

Figure 6.

The OPs in human subjects. (**A**) Extraction of the time and frequency domain OPs in a healthy adult subject. The steps are as described in Figure 1. (**B**) Mean OP power plotted as a function of frequency and intensity for healthy adult controls, adults with a history of ROP, healthy term-born infants, and age-matched infants with a history of ROP. The adult power spectra are bimodal.

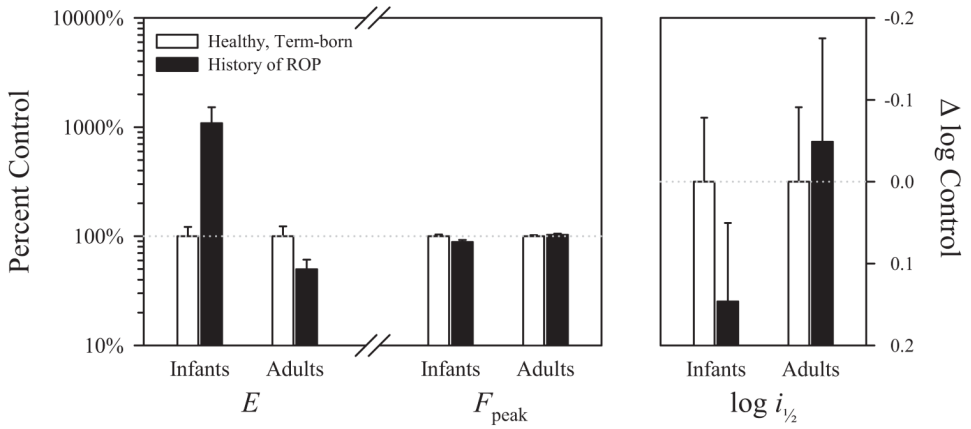

Figure 7.

Left: the frequency domain parameters OP energy (*E*) and dominant frequency (F_{peak}) are plotted for ROP subjects as a percent of normal for age. *Right*: the mean OP sensitivity (log $i_{1/2}$) is plotted as a proportion of normal. Error bars, +1 SEM.

Table 1

Parameters of Rat OPs in the Time Domain

Parameter	Intensity	Age	Control	75 Model	50/10 Model	ANOVA*
SOPA (μV)	65 R*	P20	207 (125)	209 (158)	62 (65)	F_{group} = 12.15; $P < 0.001$
		P30	171 (91)	167 (96)	113 (53)	F_{age} =3.17; $P = 0.048$
		P60	132 (83)	110 (78)	73 (42)	$F_{intensity}$ =110.03; $P < 0.001$
						$F_{group\times age}$ =2.12; $P = 0.088$
	8,500 R*	P20	425 (164)	283 (158)	121 (74)	$F_{group\times intensity}$ =11.55; $P < 0.001$
		P30	322 (99)	255 (112)	172 (91)	$F_{age\times intensity}$ =1.04; $P = 0.359$
		P60	322 (178)	225 (124)	148 (95)	$F_{group\times age\times intensity}$ =0.99; $P = 0.418$
SOPIT (ms)	65 R*	P20	218 (20)	234 (19)	224 (20)	F_{group} =0.96; $P = 0.392$
		P30	214 (19)	207 (26)	213 (16)	F_{age} =22.53; $P < 0.001$
		P60	199 (18)	192 (16)	199 (25)	$F_{intensity}$ =679.13; $P < 0.001$
						$F_{group\times age}$ =1.68; $P = 0.166$
	8,500 R*	P20	173 (18)	183 (12)	191 (17)	$F_{group\times intensity}$ =1.79; $P = 0.184$
		P30	166 (11)	164 (9)	177 (13)	$F_{age\times intensity}$ =2.89; $P = 0.063$
		P60	165 (20)	158 (13)	160 (19)	$F_{group\ age\times intensity}$ = 2.28; $P = 0.070$
Mean *IPI* (ms)	65 R*	P20	11.1 (2.6)	10.9 (1.9)	11.2 (2.2)	F_{group} =6.25; $P = 0.005$
		P30	10.4 (2.8)	9.2 (1.5)	9.9 (1.7)	F_{age} =52.73; $P < 0.001$
		P60	8.8 (4.7)	8.8 (3.1)	8.6 (2.1)	$F_{intensity}$ =11.29; $P = 0.002$
						$F_{group\times age}$ =4.65; $P = 0.002$
	8,500 R*	P20	11.3 (2.1)	11.8 (2.8)	14.1 (3.4)	$F_{group\times intensity}$ =1.44; $P = 0.252$
		P30	9.7 (1.4)	9.8 (1.9)	11.5 (2.4)	$F_{age\times intensity}$ =3.99; $P = 0.023$
		P60	10.3 (2.7)	8.7 (1.5)	9.0 (2.0)	$F_{group\times age\times intensity}$ =2.74; $P = 0.036$

Data are the mean (SD).

*Group factor is between subjects; age and intensity factors are within subjects. Significance was defined as $P < 0.05$.

Table 2

Parameters of Rat OPs in the Frequency Domain

Parameter	Intensity	Age	Control	75 Model	50/10 Model	ANOVA*
E ($\mu V^2 \cdot s^{-1}$)	65 R*	P20	3,310 (3,450)	3,730 (5,210)	610 (570)	$F_{group} = 7.24$; $P = 0.002$
		P30	2,000 (1,510)	1,730 (1,970)	710 (660)	$F_{age} = 7.08$; $P = 0.002$
		P60	1,040 (1,270)	620 (1,070)	210 (240)	$F_{intensity} = 37.73$; $P < 0.001$
						$F_{group\times age} = 1.33$; $P = 0.269$
	8,500 R*	P20	9,100 (6,330)	6,320 (7,500)	1,650 (1,430)	$F_{group\times intensity} = 7.80$; $P = 0.002$
		P30	4,920 (3,080)	2,930 (2,550)	1,690 (1,820)	$F_{age\times intensity} = 2.84$; $P = 0.065$
F_{peak} (Hz)		P60	5,240 (7,500)	1,780 (1,930)	840 (1,260)	$F_{group\times age\times intensity} = 0.86$; $P = 0.490$
	65 R*	P20	92 (16)	84 (5)	84 (12)	$F_{group} = 3.46$; $P = 0.043$
		P30	101 (14)	105 (13)	97 (12)	$F_{age} = 62.13$; $P < 0.001$
		P60	107 (16)	113 (16)	111 (17)	$F_{intensity} = 4.87$; $P = 0.034$
						$F_{group\times age} = 4.30$; $P = 0.004$
	8,500 R*	P20	91 (12)	85 (10)	77 (10)	$F_{group\times intensity} = 1.51$; $P = 0.236$
Log $i_{1/2}$ (log R*)		P30	98 (9)	101 (15)	88 (11)	$F_{age\times intensity} = 0.43$; $P = 0.651$
		P60	99 (10)	117 (9)	104 (11)	$F_{group\times age\times intensity} = 0.84$; $P = 0.507$
		P20	0.705 (0.676)	0.784 (0.574)	0.756 (0.614)	$F_{group} = 9.53$; $P < 0.001$
		P30	0.672 (0.713)	0.792 (0.561)	0.710 (0.670)	$F_{age} = 3.60$; $P = 0.033$
		P60	0.738 (0.637)	0.788 (0.568)	0.781 (0.579)	$F_{group\times age} = 0.94$; $P = 0.448$

Data are the mean (SD).

*Group factor is between subjects; age and intensity factors are within subjects. Significance was defined as $P < 0.05$.

Invest Ophthalmol Vis Sci. Author manuscript; available in PMC 2008 December 1.

Table 3

Parameters of Human OPs in the Frequency Domain

Parameter	Intensity	Group	Mean (SD)	ANOVA*
E ($\mu V^2 \cdot s^{-1}$)	65 R*	Term-born infants	80 (200)	$F_{history} = 0.01$; $P = 0.935$
		ROP infants	370 (620)	$F_{age} = 25.92$; $P < 0.001$
		Adult controls	2,840 (2,540)	$F_{intensity} = 20.94$; $P < 0.001$
		ROP adults	2,150 (2,280)	$F_{history \times age} = 11.99$; $P < 0.001$
				$F_{history \times intensity} = 0.41$; $P = 0.900$
	8,500 R*	Term-born infants	580 (780)	$F_{age \times intensity} = 4.82$; $P < 0.001$
		ROP infants	7,180 (10,180)	$F_{history \times age \times intensity} = 5.95$; $P < 0.001$
		Adult controls	17,860 (20,930)	
		ROP adults	10,020 (8,110)	
F_{peak} (Hz)	65 R*	Term-born infants	137 (35)	$F_{history} = 0.35$; $P = 0.558$
		ROP infants	146 (32)	$F_{age} = 24.81$; $P < 0.001$
		Adult controls	152 (10)	$F_{intensity} = 5.69$; $P < 0.001$
		ROP adults	147 (13)	$F_{history \times age} = 3.44$; $P = 0.067$
	8,500 R*	Term-born infants	127 (28)	$F_{history \times intensity} = 0.52$; $P = 0.817$
		ROP infants	112 (19)	$F_{age \times intensity} = 1.03$; $P = 0.412$
		Adult controls	134 (16)	$F_{history \times age \times intensity} = 2.34$; $P = 0.023$
		ROP adults	140 (14)	
Log $i_{1/2}$ (log R*)		Term-born infants	3.049 (0.484)	$F_{history} = 0.24$; $P = 0.624$
		ROP infants	3.201 (0.276)	$F_{age} = 13.34$; $P < 0.001$
		Adult controls	2.753 (0.465)	$F_{history \times age} = 0.82$; $P = 0.368$
		ROP adults	2.708 (0.546)	

*History (ROP vs. healthy) and age (adult vs. infant) factors are between subjects; intensity factor is within subjects. Significance was defined as $P < 0.05$.